**Philippine Journal of Science**
148 (1): 105-112, March 2019
ISSN 0031 - 7683
Date Received: 20 August 2018

# Modeling Adiabatic Boiling in the Biliran Geothermal Wells Using CHIM-XPT (2016)

**John Paul A. Mendoza**[1]*, **Maria Ines Rosana Balangue-Tarriela**[1], and **Mark H. Reed**[2]

[1]National Institute of Geological Sciences,
University of the Philippines Diliman, Quezon City 1101 Philippines
[2]Department of Earth Sciences, University of Oregon, Eugene, OR 97403 USA

**Boiling is a common process in geothermal wells where the primary water quickly ascends to the surface and liquid water is converted to steam due to depressurization and cools downs (*i.e.*, no heat exchange with surrounding rocks). An assumption in the present study is that there is no heat exchange between wall rock and boiling water; thus, the process is isenthalpic. This study presents the results of changes in the chemical composition of fluid from a geothermal system as it ascends to the surface together with the description of minerals precipitating out of the solution at certain temperature conditions. The results of the study will contribute significantly to the assessment of scaling potentials in a geothermal field. Using FORTRAN Programs SOLVEQ and CHIM-XPT, adiabatic boiling was simulated for the normal enthalpy wells of Biliran geothermal field. Results of theoretical geothermometry for the wells are consistent with the reported chemical geothermometers. Aside from a steam phase dominated by water vapor and $CO_2$, Well BN-1 formed chlorite, calcite (up to 170 °C) and talc in the initial boiling model. Well BN-2 precipitated mostly talc and calcite almost all throughout its ascent. The occurrence of calcite calculated from the model is consistent with the abundance of calcite scales and veins in BN-1 while BN-2 is dominated by aragonite. Minor differences in the mineralogy of the wells is mainly due to the significant difference in the fluid and gas chemistry amongst wells in the field. The partitioning of $CO_2$ into a gas phase drives the increase in pH for both wells. Both the formation of the gas phase and the fractionated minerals reflect changes occurring in the total concentration of the aqueous phase wherein species fractionated into the gas or solid phase decrease in the total aqueous concentration.**

Keywords: adiabatic boiling, Biliran Island, CHIM-XPT, geothermal, hydrothermal equilibria, whole-system geothermometry

## INTRODUCTION

As the hot geothermal fluids buoyantly rise through a fracture or an exploration or production well, the initial aqueous phase boils as a consequence of decreasing pressure. In liquid-dominated fields, this results in the separation of a gas (steam) phase from the liquid phase, which affects the pH of the rising fluids. Non-volatile components (*e.g.*, silica) remain in the liquid phase while volatile components such as $CO_2$, $N_2$, and other reduced gases ($H_2$, $CH_4$, and $H_2S$) enter the steam phase (Henley 1984, Reed 1992). Temperature of the initial liquid phase consequently decreases as fluids ascend because it takes energy to convert liquid water to steam (Reed 1992, Seward 2014). At the same time, vein and scale minerals may precipitate (*e.g.*, calcite and sulfides) and are eventually removed (fractionated) as they form, thus making the

*Corresponding author: jmendoza@nigs.upd.edu.ph

system partially open (Reed 1992). The precipitation of these minerals may pose problems (scale and blockage of formation permeability) to steam production; thus, it is important to recognize which particular minerals would form. This study in particular aims to determine the changes in the composition (chemistry, pH, *etc.*) of a particular well as fluid ascends to the surface, and to predict which minerals would precipitate out of the solution at certain temperature conditions. However, the study is limited to observing normal enthalpy neutral-Cl wells due to more complex corrections needed in reconstructing excess enthalpy wells (Arnorsson *et al.* 2007).

The study area of Biliran Island is located roughly 50 km northwest of the Greater Tongonan Geothermal Field – one of the world's largest wet-steam field. It is constructed of Quaternary volcanoes related to the subduction of the Philippine Sea Plate along the Philippine Trench and is situated along the Philippine fault zone. This setting created favorable conditions for a possible geothermal system (Pagado *et al.* 1995).

Exploration in the Biliran Island began in 1979 with the inventory of surface hydrothermal features under the Philippine National Oil Corporation – Energy Development Corporation (PNOC-EDC) and Kingston Reynolds Thom and Allardice (KRTA) Limited of New Zealand. Investigative work – including geology, geochemistry, and geophysical surveys – led to the drilling three exploratory wells (BN-1, -2, and -3 in Figure 1) from 1982 to 1983 in the Vulcan area, the site of the most impressive identified thermal area on the island. Normal enthalpy neutral-Cl fluids with $T_{SiO2}$ temperatures of 250 ºC and 210 ºC were encountered in BN-1 and -2, respectively (Ramos-Candelaria *et al.* 1993). Corrosive acid Cl-$SO_4$ water (pH = 3.0) with excess enthalpy and very high $SO_4^{2-}$, $Mg^{2+}$, and $Fe^{2+}$ was obtained from BN-3 located in the Vulcan point in the Vulcan thermal area (Apuada and Sigurjonsson 2008). Based on the current hydrogeochemical model of Biliran, neutral chloride fluid penetrates the reservoir but acidic components from magmatic sources introduced into the postulated upflow region pose a major obstacle to development. High temperatures at exploitable depths appear to be confined to a small area so no further exploration activity was taken until 1992 (Apuada and Sigurjonsson 2008). A series of geological surveys was undertaken by the PNOC-EDC Geothermal Division to reassess the significance of the geothermal areas and find alternative models to be used for assessing the feasibility of development (Pagado *et al.* 1995). In 2008, the Philippine Department of Energy

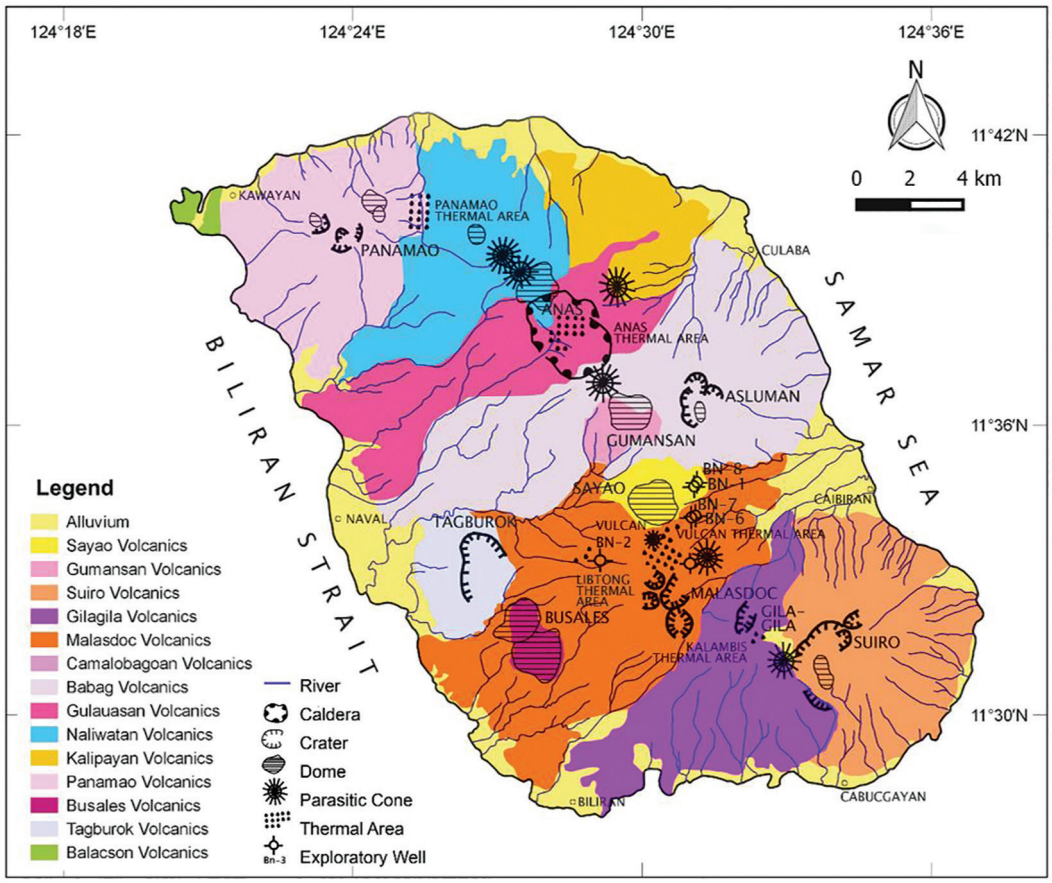


**Figure 1**. Simplified geologic map of Biliran Island (modified from FEDCO 2009).

(DOE) awarded the geothermal service contract to Biliran Geothermal Incorporated (BGI). From these previous works, four geologic units were identified on the island: (1) the metamorphic basement encountered in well BN-1, (2) the N-S folded Balacson Volcanics, (3) the Caibiran sedimentary formation encountered also encountered in BN-1, and (4) the Biliran Volcanic complex (BVC) creating most the island's landscape. Reassessment by BGI concluded the presence of at least thirteen volcanic units of BVC based on remote sensing interpretations, field stratigraphic relationship, and petrology. Figure 1 shows the distribution of volcanic features (craters, cones, caldera, and domes); thermal manifestations; exploratory wells; and geologic units.

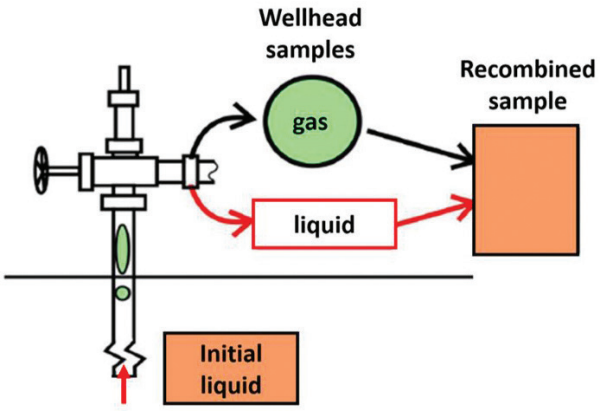


**Figure 2.** Separation of gas and liquid phase from the boiling primary well fluid as it rises can be reconstructed on the basis of thermodynamics. The composition of the primary (recombined) water is necessary for examining processes occurring at depth (modified from Reed *et al.* 2014).

## MATERIALS AND METHODS

An important assumption during geochemical modeling is that the gas and chemistry data from the well-head is representative of the reservoir fluid beneath the ground. Downhole samples may be a better representative if available, however, detailed analysis of the dissolved gas content is not measured for Biliran wells. Based on this, the result of each model depends heavily on the completeness and accuracy of the fluid and gas chemistry.

Numerical calculations were executed using the FORTRAN programs GEOCAL, SOLVEQ-XPT, and CHIM-XPT (successor of CHILLER) along with an accompanying tool called MINTAB (Reed *et al.* 2012a,b). All of these programs run in any basic command-line settings such as command prompt in Windows and use minimal computer random-access memory (RAM). GEOCAL converts parts per million (ppm) concentration into molalities and creates input files for SOLVEQ-XPT and CHIM-XPT. SOLVEQ computes the equilibrium distribution of components among aqueous species in the aqueous phase to reconstruct the initial composition of the hydrothermal fluid (primary water) in the system. For a given temperature (T) and composition (x) of a homogeneous solution, the program computes (1) activities of all aqueous species, (2) saturation indices of solids, and (3) fugacities of gases (Reed *et al.* 2012). A primary use of this program in geothermal systems is the reconstruction of the initial unboiled reservoir fluids from the well head samples, as illustrated in Figure 2. The reconstruction of the primary water is done by mixing the steam (gas) phase to the liquid phase obtained from the geothermal wells, which is a necessary step since the wellhead samples were collected after the fluids have boiled (Seward 2014). Another application of the program SOLVEQ is the computation of mineral solubility/saturation indices in the form of log (Q/K), where Q is the ion activity product or reaction quotient and K is the equilibrium constant. The technique employed by Reed and Spycher (1984) uses the log (Q/K) of different species over a range of temperatures to determine mineral equilibria. This was referred to as theoretical or whole-system chemical geothermometry. Compared to conventional geothermometers, it allows examination of the equilibrium status of the system before making a temperature estimate (Pang and Reed 1998). Plotted against temperature, as log (Q/K) curves converge to zero, the mineral assemblage in the system approaches equilibrium while curves above and below it determines the saturated and undersaturated mineral phases, respectively. Log (Q/K) plots that do not cluster at zero may represent fluids that are not in equilibrium with any subsurface mineral assemblage (Reed and Spycher 1984). Aside from this, a correction called FixAl method was applied where SOLVEQ-XPT allows force equilibration of the solution with an aluminum-bearing mineral (*e.g.*, albite, kaolinite, muscovite, *etc.*) depending on the fluid pH since aluminum is commonly not measured because its concentration is too small; thus, if detected, it may be unreliable due to this small amount. This assumption is based on the observation that hydrothermal fluids are in equilibrium with one or more aluminum-bearing minerals in most geothermal fields (Pang and Reed 1998).

The FORTRAN Program CHIM-XPT computes the equilibrium distribution of components among aqueous species, minerals, and gases at changing composition (X), pressure (P), and temperature (T). Both SOLVEQ and CHIM use equilibrium constants read from the SOLTHERM-XPT thermodynamic database. Unlike other geochemical modeling software, modeling conditions of up to 600 °C and 5 Kbar can be examined. Complex

processes including cooling hydrothermal solutions, reaction of solutions with rock, fluid-fluid mixing, gas titrations, boiling, adiabatic decompression, condensation, evaporation – as well as sedimentary (*e.g.*, diagenesis) and metamorphic processes – may be modelled using this program (Reed *et al.* 2012).

In adiabatic boiling, it is assumed that there is no heat exchange between wall rock and the boiling water. The system would have a constant enthalpy as it ascends; thus, use of the term isenthalpic. This is true for most geothermal systems since most have reached a steady-state temperature regime fixed over time by the boiling process such that wall rock temperature along the ascent path has been set by boiling itself. (Reed 1992, 1998). In this reaction, 1 kg of the primary water (reconstructed initial liquid phase from SOLVEQ) was isenthalpically boiled from the calculated or inferred reservoir temperature to the measured well head (sampling) temperature (typically near 100 °C). Incremental temperature change is then controlled to the desired interval (typically 0.01–2 °C per step). Pressure was set slightly below the calculated saturation pressure at reservoir conditions. Precipitation of kinetically-retarded minerals (*e.g.*, quartz, chalcedony, and cristobalite) is manually disallowed in the program (Reed 1992). It is also important to note that in high temperature boiling geothermal systems; redox equilibrium between the reduced gas species ($H_2$, $H_2S$, and $CH_4$); and the aqueous phase in not achieved on the time scale of boiling gas escape from liquid (Akaku *et al.* 1991). Thus, although equilibria between gas phase species and dissolved gas species are allowed, the same is not true for the following two gas-aqueous equilibria:

$$CH_4 + SO_4^{2-} = HCO_3^- + H_2O + H_2S \quad (1)$$

*(gas, aq) (aq) (aq) (aq) (aq)*

$$H_2 + 0.25SO_4^{2-} + 0.25H^+ = H_2O + 0.25HS^- \quad (2)$$

*(gas, aq) (aq) (aq) (aq) (aq)*

In order to present the data in an organized manner, an accompanying tool called MINTAB organizes the output files from SOLVEQ and CHIM. MINTAB's final output is a tabulated "flat" file that can be read by most plotting software. The different graphs created for each model are then stacked – having the same abscissa but with different distinct ordinates such as mineral abundances, gas phase composition, and concentration of aqueous component species. Table 1 and Table 2 below shows the raw data used for all the processes modeled. The dataset was obtained from Ramos-Candelaria *et al.* (1993) and was selected on the basis of completeness of routine ion and gas analysis and absence of drilling fluid contaminants in the chemistry based on Cl and Cl-$SO_4$ ratio.

## RESULTS

### Fluid Mineral Geothermometry and the FixAl Method

Representative data from the neutral wells BN-1 and BN-2 were reconstructed using SOLVEQ-XPT. Neutral-Cl separated fluid discharge from well BN1 has a laboratory pH of 8.25. With the separated gas added back into the fluid using SOLVEQ, the recalculated pH of the fluid is 5.84. Laboratory pH (quenched pH) gives clues on the molality of $H^+$ that can be added with the molalities of all derived species containing $H^+$ ($H_2S$, $HCO_3^-$, HCl, etc.) multiplied by the amount (in kg) of solvent water to get the total amount of H+ in moles – allowing the calculation of pH at any temperature indicated. Albite was used to constrain the Al concentration of the reservoir fluid. The FixAl theoretical geothermometry graph for BN1 is shown in Figure 3 where the minerals converge at a temperature of 250 °C. This is consistent with the maximum measured temperature (255 °C) and solute geothermometers (Table 3). Minerals supersaturated at lower temperature include topaz, pyrophyllite, kaolinite, heulandite, quartz, muscovite, montmorillonite, diaspore,

**Table 1**. Representative water chemistry data for Biliran geothermal wells.

| Well | Lab pH T=25 °C | Cl | $SO_4$ | $HCO_3$ | $H_2S$ | $SiO_2$ | Ca | Mg | Fe | K | Na | F | $NH_3$ | B |
|---|---|---|---|---|---|---|---|---|---|---|---|---|---|---|
| | | *Concentration in mg/kg* | | | | | | | | | | | | |
| BN-1 | 8.25 | 3650 | 106 | 1085 | 0 | 456 | 54 | 5.2 | 17.2 | 87.9 | 2736 | 31.3 | 0 | 124 |
| BN-2 | 8.4 | 2281 | 261 | 554 | 2 | 398 | 8 | 2.3 | 0.1 | 46 | 1687 | 0.85 | 1.5 | 67.5 |

**Table 2**. Representative gas chemistry data of Biliran geothermal wells.

| Well | Date | Hd | SP | $CO_2$ | $H_2S$ | $NH_3$ | RG | $N_2$ | $H_2$ | $CH_4$ |
|---|---|---|---|---|---|---|---|---|---|---|
| | | *KJ/Kg/°C* | *[MPa]* | *(mmoles/100 moles steam)* | | | | | | |
| BN-1 | 8/3/82 | 1105 | 0.300 | 2040 | 7.9 | 1.8 | 32.6 | 4.8 | 0.1 | 27.6 |
| BN-2 | 11/30/82 | 863 | 0.863 | 591 | 3.1 | 0.07 | 16.9 | 3.3 | 0.2 | 3.5 |

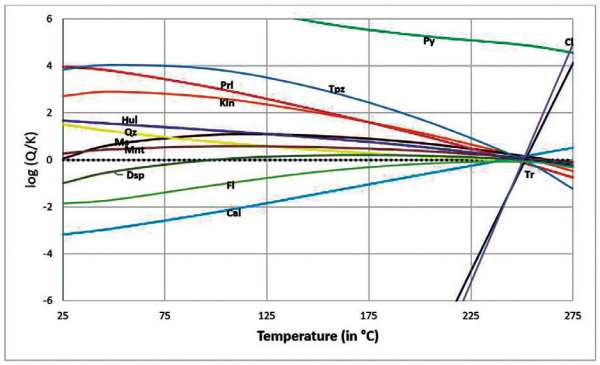


**Figure 3.** Geothermometry (FixAl graph) for well BN-1. Applying the Fix-Al method using albite, the log (Q/K) of different minerals converge at a temperature of around 250 °C – similar to previous reports. Legend: Py – pyrite, Cl – chlorite, Tr – tremolite, Tpz – topaz, Prl – pyrophyllite, Kln – kaolinite, Hul – heulandite, Qz – quartz, Ms – muscovite, Mnt – montmorillonite, Dsp – diaspore, Fl – fluorite, Cal – calcite

and fluorite. At higher temperature, chlorite-Al end member, tremolite, and calcite are supersaturated. Pyrite appears to be supersaturated at all temperature conditions.

Based on their initial pH (8.40), the reconstructed well fluids (after recombining water and gas wellhead samples using SOLVEQ) had a calculated pH of 5.57, BN-2 was force equilibrated with the muscovite to obtain an estimate of aluminum concentration in the aqueous species. Similar to well BN-1, the mineral pyrite is supersaturated throughout while minerals which increase saturation at lower temperature include mostly silica polymorphs; minerals that increase saturation at higher temperature include ankerite and pyrrhotite. The plots of log (Q/K) against temperature show a likely convergence at a temperature of around 220 °C – not far from the 206 °C bottom hole temperature measured from the well and the 210 °C estimated reservoir temperature by using silica (KRTA 1986) and Na-K-Mg geothermometers (Ramos-Candelaria *et al.* 1993), respectively. This result suggests that the fluid is in equilibrium with the hydrothermal assemblage in the wall-rock. Table 3 summarizes the different reservoir temperatures inferred from previous reports.

## Adiabatic Boiling with Mineral Fractionation

From the initial reconstructed pH of 5.82 at a likely deep reservoir temperature of 250 °C, the end pH of the fluid becomes more basic with pH 7.79 at 100 °C. At the same time, several minerals form in the initial adiabatic boiling of the reconstructed primary fluid (Figure 4A). These includes calcite; chlorite solid solution end-members (daphnite, chlinochlore, and chlorite-Mn); and minor dolomite. Calcite is the dominant mineral produced during boiling both in terms of mass and the temperature range where it precipitates (reservoir temperature to about

**Table 3**. Summary of calculated reservoir temperature for selected Biliran wells.

| | **BN-1 (2430 mTD)** | **BN-2 (2434.1 mTD)** |
|---|---|---|
| Silica geothermometry (Fournier & Potter 1982) | 250 °C[c]<br>220 °C[a,b] | 210 °C[a,b] |
| Na-K-Mg geothermometer (Giggenbach 1988) | 150 °C[c]<br>250 °C[b] | 150 °C[a]<br>210 °C[b] |
| Gas geothermometry ($T_{DAP}$)[b] | 218 °C | 255 °C |
| **Theoretical geothermometry** | **250 °C** | **220 °C** |
| Maximum measured temperature[a] | 255 °C at bottom hole after 25 days shut | 206 °C at bottom hole prior to discharge |

Notes:
[a]KRTA 1986
[b]Ramos-Candelaria *et al.* 1993
[c]FEDCO 2009

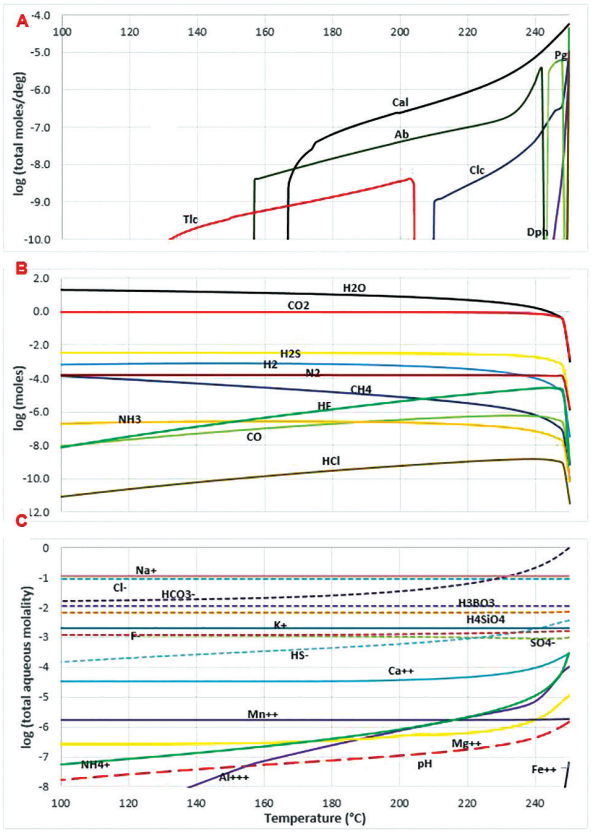


**Figure 4.** Adiabatic boiling results for BN-1 showing (A) the precipitated minerals and relative concentration in moles per °C, (B) gas concentration, and (C) molality concentration in the aqueous phase along with the pH. Abscissa of the stacked graphs all correspond to temperature in °C; thus, boiling proceeds from right to left of the graphs. Legend: Cal – calcite, Ab – albite, Prg – paragonite, Clc – clinochlore, Dph – daphnite, Tlc – talc

170 °C). As boiling proceeds (right to left in the graph), generally less chlorite is produced down to 210 °C. After cooling further, talc would start precipitating at 205 °C down to a temperature of about 130 °C. Paragonite precipitates a few degrees after initial boiling from reservoir temperature then drops out just above 240 °C. Albite appears right after paragonite disappears taking the $Na^{2+}$ and precipitates down to 155 °C. Generally, all minerals show a decrease in mass as temperature drops during boiling and are all confined in a specific range of temperature due to solubility constraints. At the same time, iron, magnesium, and aluminum is consumed by most of the silicates produced by the system (Figure 4C). The mineral assemblage becomes dominated by carbonates, magnesium (chlorite and talc), and sodium-rich silicates (albite).

During boiling, the steam phase forms and the increase in concentration is shown in Figure 4B. Large amount of an $H_2O$-$CO_2$ dominated gas phase is partitioned immediately at the beginning of boiling then generally flattens. This is followed by $H_2S$ and other minor gases. The opposite trend shown by $CH_4$ is a reflection of the disallowed equilibrium during modeling. In relation to this, the aqueous phase (Figure 4C) becomes reduced due to the escape of gases as shown in the decrease in concentration of $HS^-$ and slight increase in $SO_4^{2-}$. This is similar to the observations of Akaku *et al*. (1991). The drop in the total concentration of $HCO_3^-$ along with $Ca^{2+}$ reflects calcite precipitation.

A pH of 5.57 was computed for Well BN-2 at its reservoir temperature (210 °C). This gradually increases to a more basic pH of 7.77 upon boiling to 100 °C. Figure 5A shows the formation of kaolinite, siderite, and clinochlore on the initiation of boiling at the reservoir temperature. Kaolinite immediately depletes and replaced by chlorite (clinochlore) down to about 205 °C. Chlorite is then replaced by talc at this temperature and precipitates at a decreasing rate down to the final boiling temperature. Siderite also mimics the behavior of kaolinite and is in turn replaced by hematite, which is then replaced by talc-Fe. These Fe-rich minerals cause the depletion of $Fe^{2+}$ as shown in Figure 5C. Unlike Well BN-1, calcite is predicted to form at around 190 °C and gradually decreases in concentration until it ceases at 130 °C. At this temperature, stilbite forms at a relatively low rate down to 100 °C. In general, the mineral assemblage in the well is composed of minor iron-rich minerals (at the initial boiling temperature), calcite, and talc.

Similar to Well BN-1, the steep increase in concentration of different gases – particularly $H_2O$ and $CO_2$ (Figure 5B) – is attributed to a stronger partitioning at the start of the boiling process. Similarly, the concentration of aqueous $HCO_3^-$ decreases almost entirely due to removal into the gas phase. A small amount goes into carbonate formation. Similar trends are observed for the concentration of $Mg^{2+}$

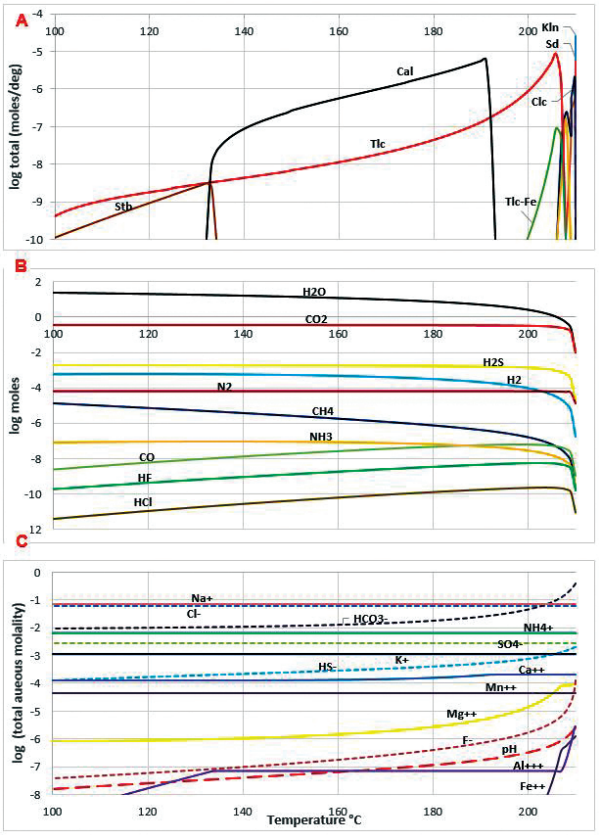


**Figure 5.** Adiabatic boiling results for BN-2 showing (A) the precipitated minerals and relative concentration in moles per °C, (B) gas concentration, and (C) molality concentration in the aqueous phase along with the pH. Abscissa of the stacked graphs all correspond to temperature in °C; thus, boiling proceeds from right to left of the graphs. Legend: Kln – kaolinite, Sd – siderite, Clc – clinochlore, Tlc-Fe – talc-Fe, Cal – calcite, Tlc – talc, Stb – stilbite

$Al^{3+}$, and $Fe^{2+}$ – which are fractionated into mineral phases.

## Model Validation

A paragenetic sequence showing the formation of different minerals precipitated through boiling simulation of the two wells is shown in Figure 5. Minerals precipitated by boiling are then compared with the observed vein minerals in the wells drilled. Generally, the predicted assemblage is comparable with the observed minerals. Except for talc, the occurrence of minerals with the highest concentration during boiling (*i.e.*, calcite, chlorite) form within the range of temperatures where these minerals were observed. Oxides such as hematite crystals, although not reflected in the figure, were also observed in the well at various depths. Kaolinite which is associated with acidic fluids was observed by other workers (Licup and Omac 2014, Reyes 2015) in narrow permeable zones of different wells.

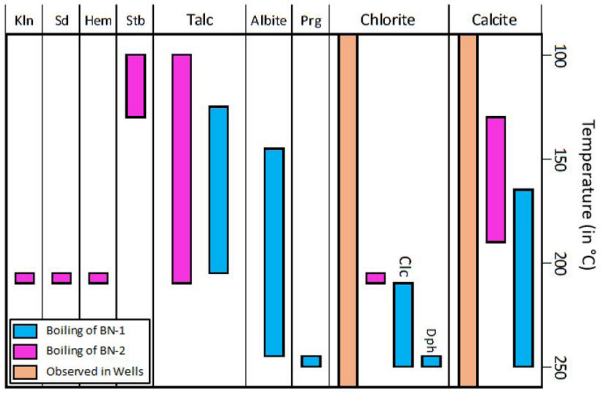


**Figure 6**. Predicted paragenetic sequence of mineral precipitation based on boiling simulations in comparison with observed temperature of occurrence of predicted minerals.

For well BN-1, calcite deposition did not occur during discharge at least within the well-bore despite its dominance in the model and an observed increase in Cl/Ca ratio through time. However, this information has not been established with any certainty due to limitations in the equipment during the time of discharge testing. On the other hand, abundant calcite is reported for cores and cuttings. FEDCO (2009) also reported the formation of a calcite blockage, which shut the well down. Instead of the predicted calcite formation, Well BN-2 deposited aragonite. KRTA (1986) attributed this abundance of aragonite to the Ca/Mg ratio. A low Ca/Mg ratio favors the more soluble aragonite due to the increased solubility of magnesium calcite.

## DISCUSSION

Results of theoretical geothermometry using the log (Q/K) for Wells BN-1 and BN-2 showed reservoir temperatures of 250 °C and 220 °C. This is consistent with the (previously) reported chemical geothermometers (silica and Na-K-Mg) and suggests that the reservoir has achieved full or partial equilibrium with the hydrothermal mineral assemblage in the reservoir.

For both wells, a large similarity was observed in the predicted assemblage. Initially, chlorites and Fe-rich rocks precipitate on boiling at reservoir temperature. As the boiling fluid cools down, other significant minerals such as calcite and talc precipitate at a certain temperature range then gradually decreases in amount. In particular, the abundance of calcite in well scales and veins for BN-1 gives a relatively high confidence in the accuracy of the model, which can be further improved if rock cuttings and cores become available. Minor differences in the mineralogy of the wells is mainly due to the significant difference in the fluid and gas chemistry, which can readily be noticed at Table 1 and Table 2. Knowing this information, scaling problems might be a problem for the wells; thus, there is a need to plan for interventions which can prevent its formation.

Both of the neutral wells of Biliran show an increasing pH trend as boiling proceeds. This change in pH is consistent with that observed by Reed (1992) for neutral wells and is mainly driven by the escape of $CO_2$ to the gas phase – as shown in Equation 3. At the same time, both cases show a relatively steep change in pH at the onset of boiling then gradually flatten due to the stronger partitioning of $CO_2$ at this stage. In general, partitioning of different gases is strongest at the start of boiling.

$$\underset{(aq)}{HCO_3} + \underset{(aq)}{H^+} = \underset{(q)}{CO_2} + \underset{(aq,\,g)}{H_2O} \qquad (3)$$

Both the formation of the gas phase and mineral fractionation is reflected in changes occurring in the concentration of the aqueous phase. Generally, species that fractionate into the gas or solid phase show a decrease in aqueous concentration.

It is recommended to continue further studies such as models on other hydrothermal processes explaining the high dissolved iron in Biliran well fluids despite being a neutral well.

## ACKNOWLEDGMENTS

The authors would like to thank the host company BGI for access to all important data needed for this study. They would also like to thank the UP Diliman OVCRD and Office of International Linkages – UP System for the additional funds needed for the software training.

## REFERENCES

AKAKU K, REED MH, YAGI M, KAI K, YASUDA Y. 1991. Chemical and Physicals Processes Occurring in the Fushime Geothermal System, Kyushu, Japan. Geochemical Journal 25: 315–333.

APUADA NA, SIGURJONSSON GF. 2008. The Geothermal Potential of Biliran Island, Philippines. Proceedings of the 8th Asian Geothermal Symposium; 09–10 Dec 2008; Vietnam Institute of Geosciences and Mineral Resources (VIGMR), Hanoi City, Vietnam. p. 73–77.

ARNORSSON, STEFANSSON A, BJARNASON JO. 2007. Chapter 9: Fluid-Fluid Interactions in

Geothermal Systems. In: Richards J, Larson P eds. Fluid-Fluid Interactions. Reviews in Mineralogy and Geochemistry 65: 259–312.

[FEDCO] FILTECH Energy Drilling Corporation. 2009. Resource Assessment: The Biliran Geothermal Field, Philippines [Internal Report]. Biliran Geothermal Incorporated (BGI). 184p.

FOURNIER, RO, POTTER RW. 1982. A Revised and Expanded Silica (Quartz) Geothermometer. Geothermal Resources Council Bulletin 11: 3–12.

GIGGENBACH WF. 1988. Geothermal solute equilibria derivation of Na-K-Mg-Ca geoindicators. Geochimica et Cosmochimica Acta 52: 2749–65.

HENLEY RW. 1984. Chapter 2. In: Robertson J ed. Fluid-Mineral Equilibria in Hydrothermal Systems. Reviews in Economic Geology 1: 9–28.

[KRTA] Kingston Reynolds Thom & Allardice Limited. 1986. Evaluation of the Biliran Geothermal Prospect [Internal Report]. Philippine National Oil Company – Energy Development Corporation (PNOC-EDC). 128p.

LICUP AC, OMAC XL. 2014. Geology of BN-6 [Unpublished Company Report]. Biliran Geothermal Incorporated. 52p.

PAGADO ES, CAMIT GRA, ROSELL JB, APUADA NA. 1995. The Geology and Geothermal Systems of Biliran Island. Journal of the Geological Society of the Philippines 5(1): 21–36.

PANG ZH, REED MH. 1998. Theoretical Chemical Geothermometry on Geothermal Waters: Problems and Methods. Geochimica Cosmochimica Acta 62(6): 1083–91.

RAMOS-CANDELARIA MN, RUAYA JR, BALTASAR ASJ. 1993. Geochemical and Isotopic Investigation of Biliran Geothermal Discharges, Philippines. Proceedings of the final Research Co-ordination Meeting on the Application of Isotope and Geochemical Techniques to Geothermal Exploration in the Middle East, Asia, the Pacific and Africa. 12–15 Oct 1993; Dumaguete City, Philippines. p. 169–184.

REED MH. 1992. Computer Modeling of Chemical Processes in Geothermal Systems: Examples of Boiling, Mixing and Water-Rock Reaction. In: D'Amore F ed. Application of Geochemistry in Geothermal Reservoir Development. New York (USA): United Nations Institute for Training and Research. p. 275–298.

REED MH. 1998. Chapter 5: Calculation of Simultaneous Chemical Equilibria in Aqueous-Mineral-Gas Systems and its Application to Modeling Hydrothermal Processes. In: Richards J, Larson P eds. Techniques in Hydrothermal Ore Deposits Geology. Reviews in Economic Geology 10: 109–124.

REED MH, SPYCHER NF. 1984. Calculations of pH and mineral equilibria in hydrothermal waters with application to geothermometry and studies of boiling and dilution. Geochimica Cosmochima Acta 48: 1479–92.

REED MH, SPYCHER NF, PALANDRI J. 2012a. SOLVEQ-XPT: A Computer Program for Computing Aqueous-Mineral-Gas Equilibria. Eugene, OR: Department of Geological Sciences, University of Oregon. 41p.

REED MH, SPYCHER NF, PALANDRI J. 2012b. Users Guide for CHIM-XPT: A Program for Computing Reaction Processes in Aqueous-Mineral-Gas Systems and MINTAB Guide (Version 2.43). Eugene, OR: Department of Geological Sciences, University of Oregon. 71p.

REED MH, PALANDRI J, CLEMENTE V, CABAHUG R. 2014. Computation of reservoir geochemical conditions from excess-enthalpy wellhead samples. Portland, OR (USA): Geothermal Resources Council Transactions; 28 Sep – 01 Oct 2014. p. 461–463.

REYES AG. 2015. A Petrological Evaluation of Well BN-6D. GNS Science Consultancy Report No. 2015/105. 10p.

SEWARD RJ. 2014. Geothermal Fluid Equilibrium Modeling: Comparison of Wellhead Fluid Samples to Deep Samples in the Reykjanes System, Iceland. [MS Thesis]. Eugene, OR: University of Oregon. 61p.